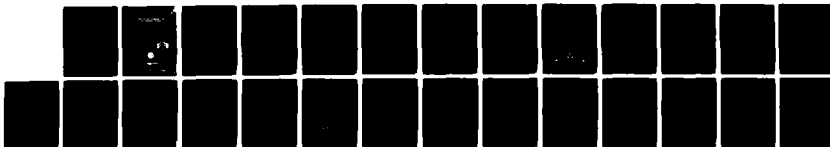


AD-A121 345 DOPPLER PROPERTIES OF POLYPHASE CODED PULSE COMPRESSION 1/0
WAVEFORMS(U) NAVAL RESEARCH LAB WASHINGTON DC
F F KRETSCHMER ET AL. 30 SEP 82 NRL-8635

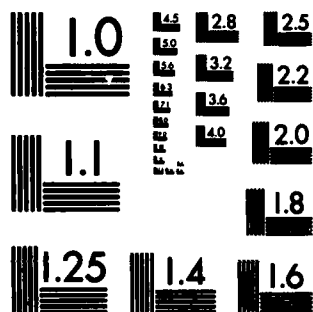
UNCLASSIFIED

F/G 9/4

NL



END
DATE
FILMED
DTIC



MICROCOPY RESOLUTION TEST CHART
NATIONAL BUREAU OF STANDARDS-1963-A

AD A121345

REPORT DOCUMENTATION PAGE		READ INSTRUCTIONS BEFORE COMPLETING FORM
1. REPORT NUMBER NRL Report 8635	2. GOVT ACCESSION NO. AD-A121345	3. RECIPIENT'S CATALOG NUMBER
4. TITLE (and Subtitle) DOPPLER PROPERTIES OF POLYPHASE CODED PULSE COMPRESSION WAVEFORMS		5. TYPE OF REPORT & PERIOD COVERED Interim report on a continuing NRL problem.
		6. PERFORMING ORG. REPORT NUMBER
7. AUTHOR(s) F. F. Kretschmer, Jr. and B. L. Lewis		8. CONTRACT OR GRANT NUMBER(s)
9. PERFORMING ORGANIZATION NAME AND ADDRESS Naval Research Laboratory Washington, DC 20375		10. PROGRAM ELEMENT, PROJECT, TASK AREA & WORK UNIT NUMBERS 62712N SF12-131-691 53-0605-0-2
11. CONTROLLING OFFICE NAME AND ADDRESS Naval Sea Systems Command Washington, DC 20362		12. REPORT DATE September 30, 1982
		13. NUMBER OF PAGES 25
14. MONITORING AGENCY NAME & ADDRESS (if different from Controlling Office)		15. SECURITY CLASS. (of this report) UNCLASSIFIED
		15a. DECLASSIFICATION/DOWNGRADING SCHEDULE
16. DISTRIBUTION STATEMENT (of this Report) Approved for public release; distribution unlimited.		
17. DISTRIBUTION STATEMENT (of the abstract entered in Block 20, if different from Report)		
18. SUPPLEMENTARY NOTES		
19. KEY WORDS (Continue on reverse side if necessary and identify by block number) Radar Waveforms Pulse compression Coding		
20. ABSTRACT (Continue on reverse side if necessary and identify by block number) Doppler properties of the Frank polyphase code and the recently derived P1, P2, P3, and P4 polyphase codes are investigated and compared. An approximately 4 dB cyclic variation of the peak compressed signal is shown to occur as the doppler frequency increases. The troughs in the peak-signal response occur whenever the total phase shift, due to doppler, across the uncompressed pulse is an odd multiple of π radians. It is shown that, although the P3 and P4 codes have larger		

(Continued)

DD FORM 1473
1 JAN 73EDITION OF 1 NOV 69 IS OBSOLETE
S/N 0102-014-6601

SECURITY CLASSIFICATION OF THIS PAGE (When Data Entered)

20. ABSTRACT (Continued)

zero-doppler peak sidelobes than the other codes, the P3 and P4 codes degrade less as the doppler frequency increases. Also, the effects of amplitude weighting and receiver bandlimiting for both zero and nonzero doppler are investigated.

CONTENTS

INTRODUCTION	1
PROPERTIES OF POLYPHASE-CODED WAVEFORMS	1
Frank Polyphase-Coded Waveforms	1
Effects of Band-Limiting Frank-Coded Waveform Prior to Pulse Compression	5
P1, P2, P3, and P4 Polyphase Codes	6
DOPPLER PROPERTIES OF POLYPHASE CODES	7
Ambiguity Functions and Cyclic Losses	7
FFT Implementations and Doppler Compensation	11
Comparison of Doppler Responses and Effects of Weighting	12
Band-Limiting Effects on Doppler Responses	15
SUMMARY	22
ACKNOWLEDGMENT	22
REFERENCES	22

Accession For	
NTIS GRA&I	<input checked="" type="checkbox"/>
DTIC TAB	<input type="checkbox"/>
Unannounced	<input type="checkbox"/>
Justification	
Distribution/	
Availability Codes	
Dist	Avail and/or Special
A	

DOPPLER PROPERTIES OF POLYPHASE CODED PULSE COMPRESSION WAVEFORMS

I. INTRODUCTION

The Frank polyphase-coded waveform and the P1, P2, P3, and P4 polyphase pulse-compression waveforms previously described by the authors [1-3] provide a class of frequency-derived phase-coded waveforms that can be sampled upon reception and processed digitally. These waveforms are derivable from the chirp and step-chirp analog waveforms and are therefore similar in certain respects. There are some important differences, however, which include differences in sidelobe levels, implementation techniques and doppler characteristics.

The compressed pulse of the polyphase-coded waveforms has sidelobes which decrease as the pulse compression ratio ρ is increased. For ρ equal to 100, the peak sidelobes range from 26 to 30 dB below the peak signal response, depending on the particular code. In contrast, the compressed chirp or step-chirp pulse has approximately 13 dB sidelobes, independent of the pulse compression ratio, which can mask a relatively weak nearby target. An amplitude weighting is generally applied to reduce the sidelobes and the resulting mismatch reduces the output S/N by 1 to 2 dB.

The polyphase-coded waveforms are capable of large pulse-compression ratios, which may be efficiently implemented using the phase shifts provided by a fast Fourier transform (FFT). Thus, the FFT can be used directly as the pulse compressor. These waveforms can also be efficiently compressed with another pulse-compression technique in which the FFT is used to convert to the frequency domain, where the matched filtering and weighting are performed. This processing is followed by an inverse FFT to restore the signal to the time domain.

This report first reviews the properties of the polyphase-coded waveforms, then it focuses on the doppler characteristics of these waveforms. A cyclic loss of approximately 4 dB is discussed which is characteristic of frequency-derived polyphase-coded waveforms having low sidelobes. This cyclic variation was not recognized in the prior literature dealing with Frank codes [4,5]. A method of compensating for this loss is described.

The doppler characteristics of the various polyphase codes are investigated in detail. Also, the effects of weighting on the doppler performance of the codes is presented. This weighting may be due to an applied amplitude weighting and/or it may be caused by bandlimiting in the receiver.

PROPERTIES OF POLYPHASE-CODED WAVEFORMS

Frank Polyphase-Coded Waveforms

The Frank polyphase-coded waveform may be described and generalized by considering a hypothetically sampled step-chirp waveform [1,2]. The Frank code was not originally described in this manner but was given in terms of the elements of a matrix [6]. As an example, consider a four-frequency step-chirp waveform, as shown in Fig. 1(b), where the F_i 's denote frequency tones. In this waveform, the frequency steps are equal to the reciprocal of the tone duration $4\tau_c$, where τ_c denotes

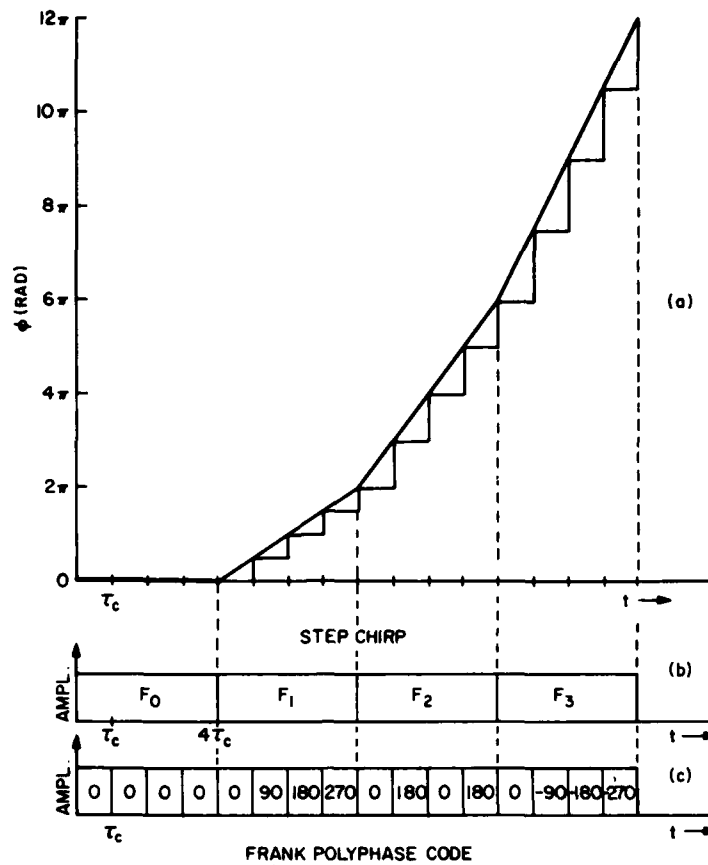


Fig. 1 — Step-chirp and Frank-polyphase-code relationships

the compressed pulsewidth. Assuming that this waveform has been beat to the baseband in-phase (I) and quadrature (Q) components using a synchronous oscillator having a frequency the same as the first tone frequency, the resultant phase-vs-time characteristic consists of four linear sections as shown on Fig. 1(a). The corresponding baseband frequencies are the subharmonics of the frequency $1/\tau_c$. If the baseband phases of the step-chirp waveforms are sampled every τ_c s and held for τ_c s, the phase sequence shown in Fig. 1(c) is obtained. This sequence of phases constitutes the phases of a Frank code for $N = 4$, corresponding to the four baseband frequencies of the hypothetical step-chirp waveform. The actual transmitted Frank-coded waveform consists of a carrier whose phase is modulated according to the indicated baseband waveform sequence. For each frequency, or section, of the step-chirp phase characteristic, a phase group consisting of N phase samples is obtained and the total number of code phases is N^2 , which is equal to the pulse-compression ratio. Note that the phase increments within the four phase groups are 0° , 90° , 180° , and 270° . However, the phases of the last group are ambiguous ($> 180^\circ$) and appear as -90° phase steps or as the conjugate of the F_1 group of phases, which corresponds to the lower sideband of F_1 . The last group of phases appears, because of the ambiguity, to complete one 360° counterclockwise rotation rather than the $(N - 1)$ rotations of the end frequency of the step-chirp waveform.

The Frank-code phases may be stated mathematically as follows. The phase of the i th code element in the j th phase group, or baseband frequency, is

$$\phi_{i,j} = (2\pi/N)(i - 1)(j - 1), \quad (1)$$

where the index i ranges from 1 to N for each of the values of j ranging from 1 to N . An example of a brute force Frank-code pulse generation for $N = 3$ is shown in Fig. 2. The Frank-code phases are the same as the negative of the steering phases of an N -point DFT, where the j th frequency coefficient is

$$F_j = \sum_{i=1}^N a_i \exp[-j2\pi(i-1)(j-1)/N], \quad (2)$$

where a_i is the i th complex input time sample. This means that a considerable savings in hardware can be achieved by using the efficiency of an FFT.

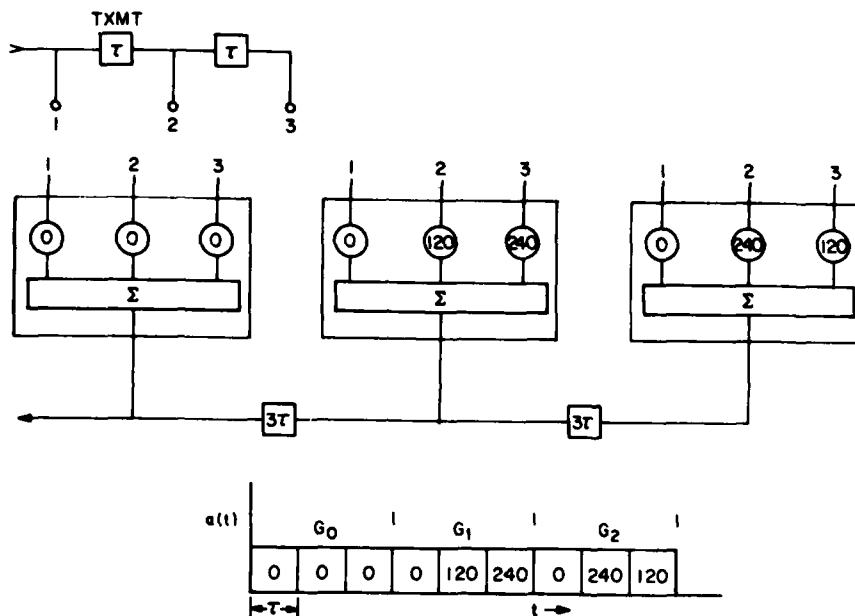


Fig. 2 — Simplified Frank-code generation

The matched-filter output for an $N = 10$ (100-element) Frank code is shown in Fig. 3. This figure and the following figures showing the compressed pulse were obtained by sampling the input baseband waveform once per code element or per reciprocal bandwidth unless stated otherwise. With a discrete-time matched filter, the output signal is also a discrete-time sampled signal. However, for ease of plotting and viewing the points were connected by straight lines. The four sidelobe peaks on each half of the match point (peak response) are of equal magnitude. The first peak sidelobe, at sample number 5 in Fig. 3, occurs as the last phase group having -36° phase increments indexes halfway into the first phase group of zero phase vectors in the autocorrelation process. In general, at sample number $N/2$ there are $N/2$ vectors adding to complete a half circle. The end phase group indexing into the first phase group of 0° vectors approximates a circle, since the phases of the last phase group make only one rotation as stated previously. The peak sidelobe amplitude may be approximated by the diameter D of the circle from the relation

$$\text{Perimeter} = N = \pi D \quad (3)$$

or

$$D = N/\pi. \quad (4)$$

At the match point the amplitude is N^2 , so that the peak-response to peak-sidelobe power ratio R is

$$R = \frac{N^4}{(N/\pi)^2} = N^2\pi^2 = \rho\pi^2. \quad (5)$$

For a 100-element Frank code, this ratio is approximately 30 dB, as shown in Fig. 3.

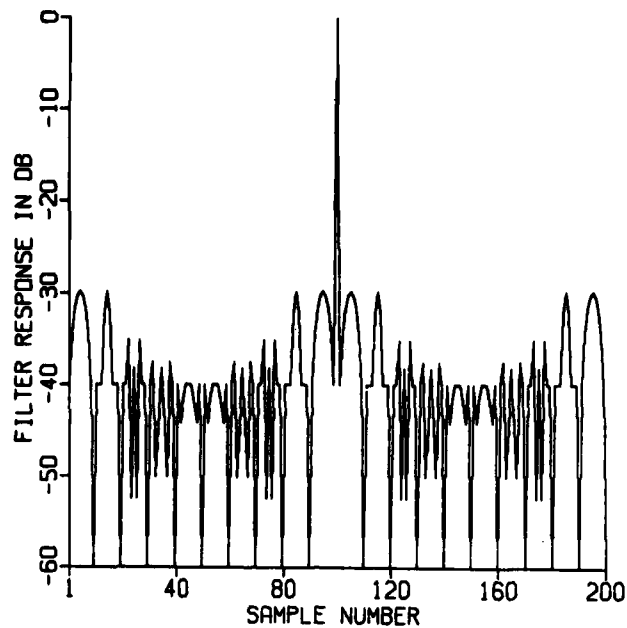


Fig. 3 — Compressed pulse of 100-element Frank code

Had the phases of the polyphase-coded waveform been generated by use of the phases of the step-chirp phase characteristic sampled at one-fifth of the interval used for the Frank code, the compressed code would appear as shown in Fig. 4. In this figure, five samples are equal in time to one sample in Fig. 3. Note in Fig. 4 that the near-in sidelobes are approximately 13 dB and that the envelope of the sidelobe peaks is approximately that of a $\sin x/x$ pulse. The 13-dB sidelobes also appear for an oversampling of 2:1. These comments also apply to the other polyphase codes described in this report. Also, note that the compressed pulsewidth in Fig. 4 has not decreased, since it is determined by the underlying bandwidth of the step-chirp waveform.

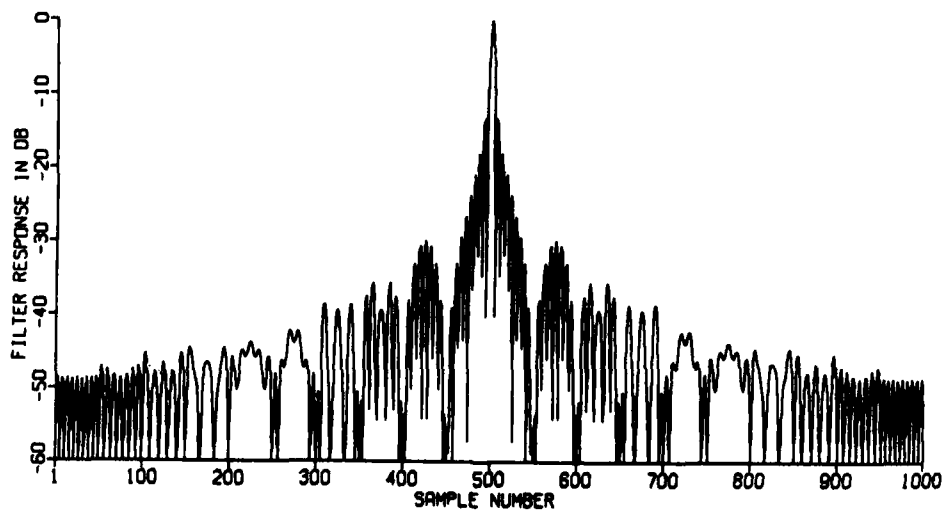


Fig. 4 — Compressed pulse of oversampled (5:1) step-chirp

Effects of Band-Limiting Frank-Coded Waveform Prior to Pulse Compression

A Frank-coded waveform is depicted in Fig. 5(a), where the G_K 's denote the phase groups corresponding to the sampled phases of a step-chirp waveform as previously discussed. Each group consists of N vectors beginning with a vector at a phase angle of 0° . The phase increments within the K th group are

$$\Delta\phi_K = K \frac{360^\circ}{N}. \quad (6)$$

Thus G_0 consists of N vectors at 0° , G_1 has vectors separated by $360^\circ/N$, and so forth, until at the center of the coded waveform the phase increments approach 180° or become 180° , depending on whether N is odd or even. For phase increments greater than 180° the phases are ambiguous, with the result that the phasors of phase group G_{N-K} are the conjugates of the phasors of phase group G_K , so that the vectors have the same increments but rotate in opposite directions. The result is that the phase increments are small at the ends of the code and become progressively larger toward the center of the code, where the increments approach 180° from opposite directions.

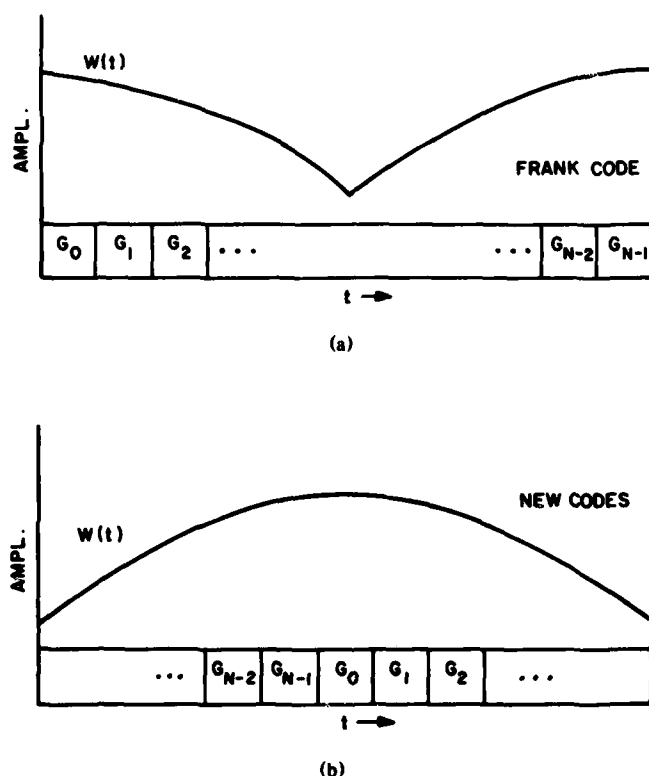


Fig. 5 — Effect of band limiting before pulse compression

If a receiver is designed so that it has an approximately rectangular bandwidth corresponding to the 3-dB bandwidth of the received waveform, the received waveform becomes bandlimited and a mismatch occurs with the compressor. This band limiting would normally occur prior to sampling in the analog-to-digital (A/D) conversion process to prevent noise foldover and aliasing. The result of any band limiting is to average (or smooth) the vectors constituting the coded waveform, and for the

Frank code a weighting $W(r)$ such as illustrated in Fig. 5(a) takes place due to the larger phase increments toward the middle of the code. This weighting causes an unfavorable mismatch with the compressor, which results in a degradation of the sidelobes relative to the peak response.

The new symmetrical codes found by the authors have the common property that the phase groups with the small phase increments are at the center of the code and the larger-increment groups progress symmetrically toward the ends of the code. This is illustrated in Fig. 5(b), where a favorable amplitude weighting resulting from band limiting prior to pulse compression is shown.

P1, P2, P3, and P4 Polyphase Codes

The new polyphase codes which tolerate band limiting are referred to as the P1, P2, and P4 codes. The P1 code was derived from use of the previously described relationship between the Frank-code phases and those of a sampled step-chirp waveform. The desired symmetry, with the dc or small incremental phase group at the center of the code, can be achieved from a determination of the phases that result from placing the hypothetical synchronous oscillator at the band center of the step-chirp waveform. For an odd number of frequencies, the synchronous oscillator frequency corresponds to one of the waveform frequencies and the resultant phases are the same as for the Frank code, except that the phase groups are rearranged as indicated in Fig. 5(b). If there is an even number of frequencies, the synchronous oscillator frequency placed at the band center does not correspond to one of the frequencies in the step-chirp signal. The phase of the i th element of the j th group is given in degrees by

$$\phi_{i,j} = - (180/N) [N - (2j - 1)] [(j - 1)N + (i - 1)], \quad (7)$$

where i and j are integers ranging from 1 to N .

The P2 code, which also has the desired features, is similar to the Butler-matrix steering phases used in antennas to form orthogonal beams. The P2 code is valid for N even, and each group of the code is symmetric about 0° phase. The usual Butler-matrix phase groups are not symmetric about 0° phase and result in higher sidelobes. For N even, the P1 code has the same phase increments, within each phase group, as the P2 code, except that the starting phases are different. The i th element of the j th group of the P2 code is given in degrees by

$$\phi_{i,j} = (90/N) (N + 1 - 2i) (N + 2 - 2j), \quad (8)$$

where i and j are integers ranging from 1 to N as before. The requirement for N to be even in this code stems from the desire for low autocorrelation sidelobes; an odd value for N results in high autocorrelation sidelobes. This code has the frequency symmetry of the P1 code and also has the property of being a palindromic code, which is defined as a code having symmetry about the center.

The P4 code is similar to the P1 code, except that the phase samples are those of a sampled chirp waveform rather than a step-chirp waveform. In each case, the synchronous oscillator is placed at the band center, with the result that the codes are symmetrical. The P3 code is also derived from a chirp waveform and is the counterpart of the Frank code where the synchronous oscillator is put at the lowest frequency to determine the phases. The P3 code, like the Frank code, is therefore intolerant of band limiting.

The phases of a modified P4 code* are given by

$$\phi_i = (45/\rho) (2i - 1)^2 - 45(2i - 1), \quad 1 \leq i \leq \rho, \quad (9)$$

and the phases of the P3 code are

$$\phi_i = (180/\rho) (i - 1)^2, \quad 1 \leq i \leq \rho. \quad (10)$$

*This code varies slightly from the one given in [3]. In effect, the first sample of the Nyquist sampling of a chirp signal has been shifted by half a sample period to produce a palindromic code.

The compressed pulse for a 0-doppler, 100-element P3 or P4 code is shown in Fig. 6. It is similar to the Frank, P1, and P2 100-element codes, except that the peak sidelobes are approximately 4 dB higher.

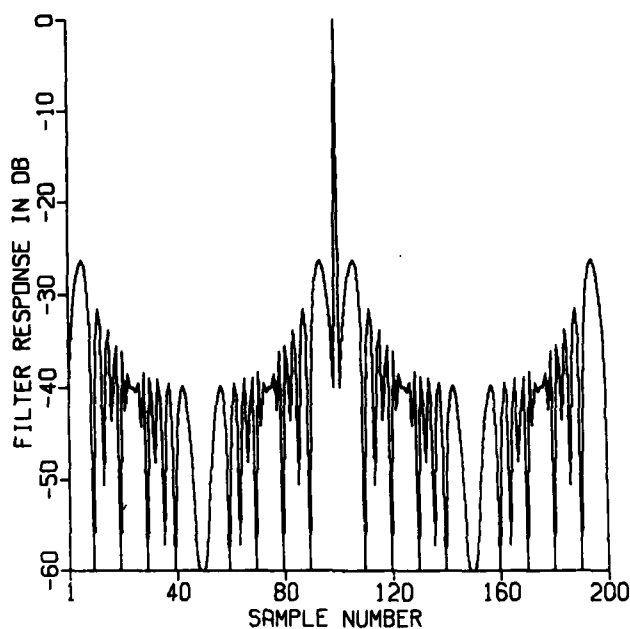


Fig. 6 — Compressed pulse of 100-element P3 or P4 code

DOPPLER PROPERTIES OF POLYPHASE CODES

Ambiguity Functions and Cyclic Losses

A partial ambiguity function for a 100-element Frank code is shown in Fig. 7, which shows the amplitude in dB of a matched-filter output for given doppler shifts of the input. The doppler is normalized to the signal bandwidth and the delay axis is normalized to the uncompressed pulse length. The cut through this diagram at 0 doppler shows the output of a perfectly matched receiver. In this case, the output pulse is the same as the autocorrelation function of the input waveform. A cut along any other doppler axis shows the output of the receiver for an input waveform having a doppler which is mismatched to the receiver by the stated amount. The vertical scale ranges from 0 dB to -60 dB, and the -30 dB sidelobes for 0 doppler are evident. The normalized doppler shift of -0.05 shown in this figure corresponds to a mach-50 target for an L-band radar having a signal bandwidth of 2 MHz. The first doppler cut shown in the literature [4] is taken at this normalized doppler, and the resultant high-peak sidelobes shown in Fig. 8 have perhaps discouraged usage of the Frank code. The region shown in Fig. 7 between 0 and -0.005 doppler (mach-5), with a delay interval of ± 0.3 , is of interest, and it is shown on an expanded scale in Fig. 9. In this region, the doppler response is good in terms of the sidelobe levels. (The blank spot on the plot was caused by a computer plotting glitch.) The corresponding ambiguity function for the 100-element P4 code is shown in Fig. 10, where the peak response is seen to have the same cyclic variation as the Frank code. The differences between these ambiguity functions will be discussed in later sections, and it will be shown that amplitude weighting or band limiting will reduce the image lobes at the ends of the compressed pulse. At a doppler shift of -0.005, or more generally $\pm 1/(2p)$, the total phase shift across the uncompressed pulse is π and the peak response drops approximately 4 dB. At this doppler, there is a range-doppler coupling of half a

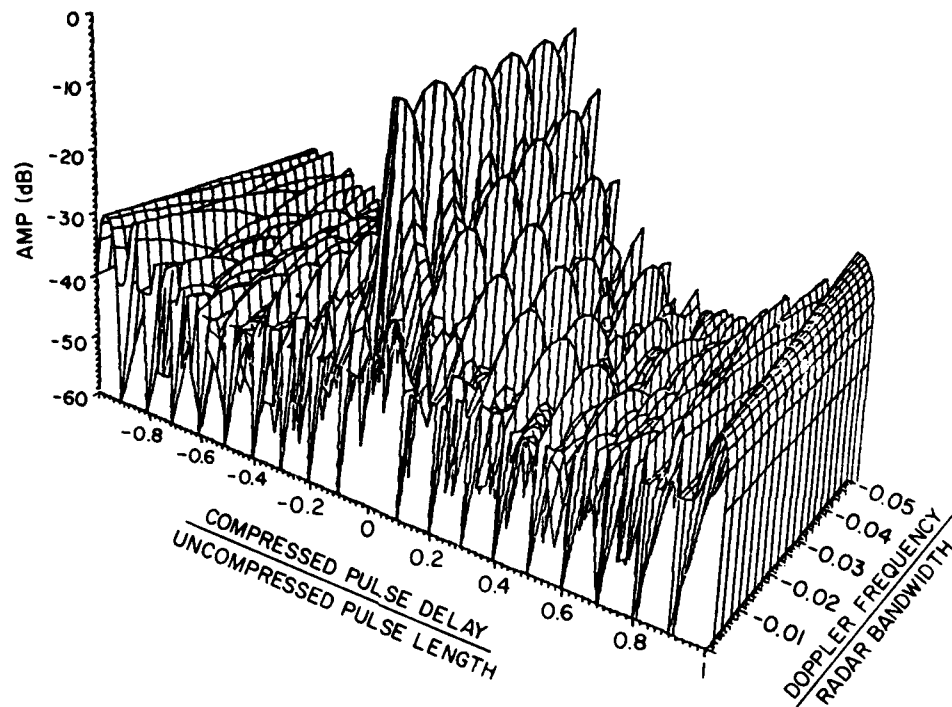


Fig. 7 — Partial ambiguity function for 100-element Frank code

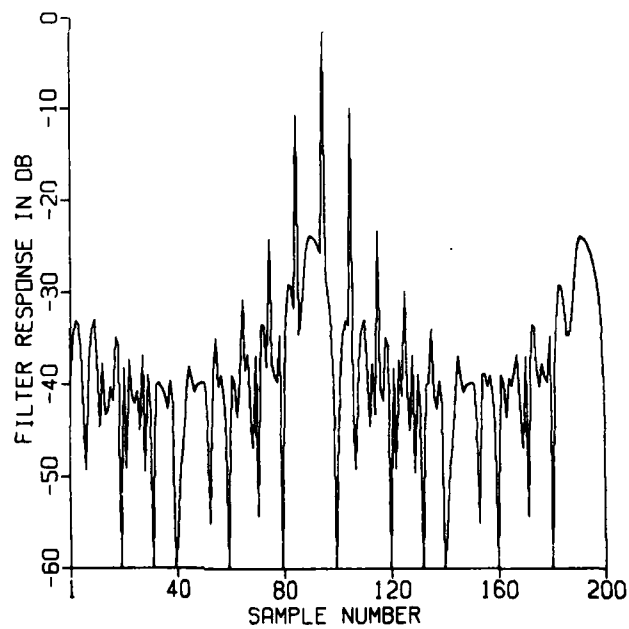


Fig. 8 — Compressed pulse of 100-element Frank code.
doppler = -0.05

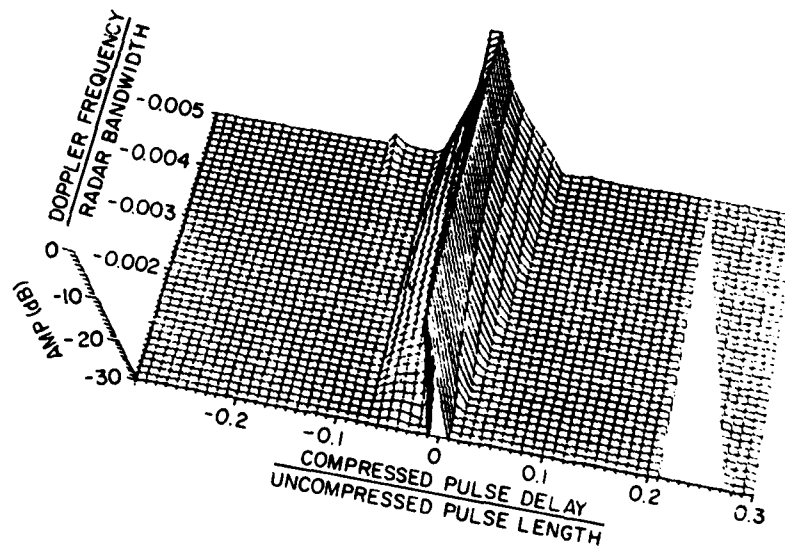


Fig. 9 — Magnified ambiguity function of 100-element Frank code

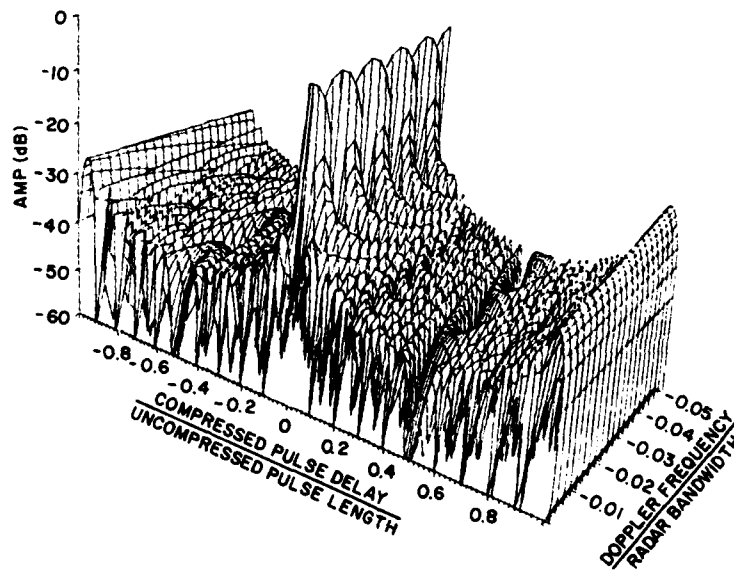


Fig. 10 — Partial ambiguity function for 100-element P4 code

range cell, with the result that the signal splits between two range cells. This is illustrated in Fig. 11 for the Frank code. At a normalized doppler shift of -0.01 , or in general $\pm 1/\rho$, there is a range-doppler coupling of one range cell resulting from a total phase shift of 2π radians across the uncompressed pulse, and the main peak response is restored to nearly full amplitude as shown in Figs. 7 and 10. This effect is cyclic and a loss of approximately 4 dB is encountered when the total phase shift due to doppler is an odd multiple of 180° .

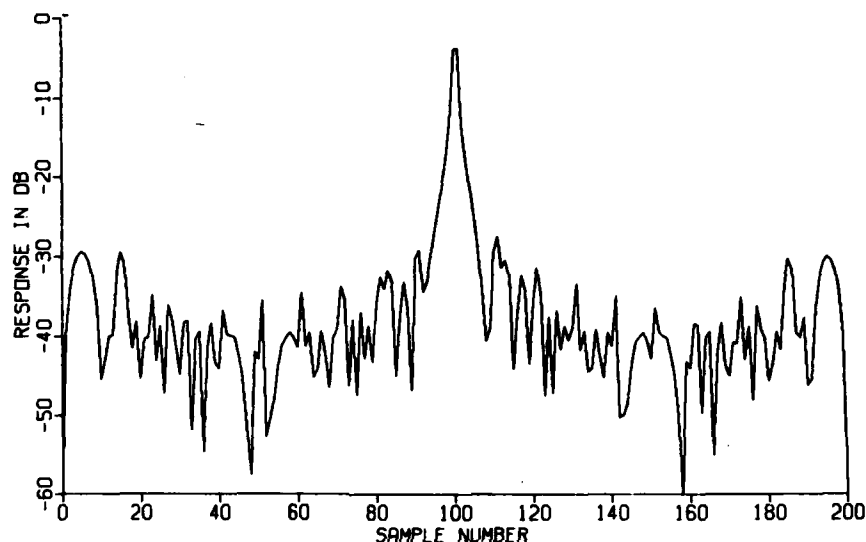


Fig. 11 — Compressed pulse of 100-element Frank code,
doppler = -0.005

The loss may also be shown if we consider the misalignment of the vectors at the pulse compressor output due to a doppler shift which results in phase shifts across the uncompressed pulse duration T . The loss occurs because the matched filter does not desteer the phases due to doppler. For a doppler frequency f_d , the phase increments from subpulse to subpulse are

$$\Delta\theta = 2\pi f_d T / \rho, \quad (11)$$

and the resultant unit-normalized signal is

$$\begin{aligned} S &= \frac{1}{\rho} \sum_{n=0}^{\rho-1} e^{-jn\Delta\theta} \\ &= \frac{1}{\rho} \frac{\sin \rho(\Delta\theta/2)}{\sin (\Delta\theta/2)}. \end{aligned} \quad (12)$$

For $\Delta\theta = 0$, the maximum normalized output of one is obtained. When the total phase shift across the uncompressed pulse is π , one finds that

$$S = 2/\pi. \quad (13)$$

This is equivalent to an approximately 4 dB loss and corresponds to a range-doppler coupling of half a range cell. As mentioned previously, for a range-doppler coupling of one range cell, the total phase shift across the uncompressed pulse is 2π and the peak amplitude is nearly restored. The trough following each peak is down approximately 4 dB from the peak.

It should be noted that this 4-dB loss also occurs in a pseudorandom binary shift register code when the doppler phase shift across the uncompressed pulse is π . However, the response is not cyclic and monotonically decreases as the doppler frequency is increased. For this reason, a doppler filter bank is usually instrumented to cover the doppler band of interest.

The cyclic loss indicated for the polyphase code is a consequence of deriving the phases of the polyphase code from those of a step-chirp or chirp waveform sampled at the Nyquist rate. Had the phases been sampled faster, the cyclic loss would decrease and the peak sidelobes of the compressed pulse would increase to approximately 13 dB as previously described. This is a general property of the polyphase codes described in this report.

FFT Implementations and Doppler Compensation

Another property of the polyphase codes described in this report is that they can be implemented with a modified FFT phase structure. An example is shown in Fig. 12 for a P1 code. Each code can be generated or compressed with the same standard FFT phase filter shown in Fig. 13. The phase shifts used before and after the FFT phase filter depend on the particular code.

One way to reduce the 4-dB cyclic variation of the polyphase codes is to provide an additional output port for the compressed pulse which provides an approximate phase compensation of π . This could be achieved by the use of additional phase shifters and delay lines in the F_i output ports of the FFT phase filter shown in Fig. 12.

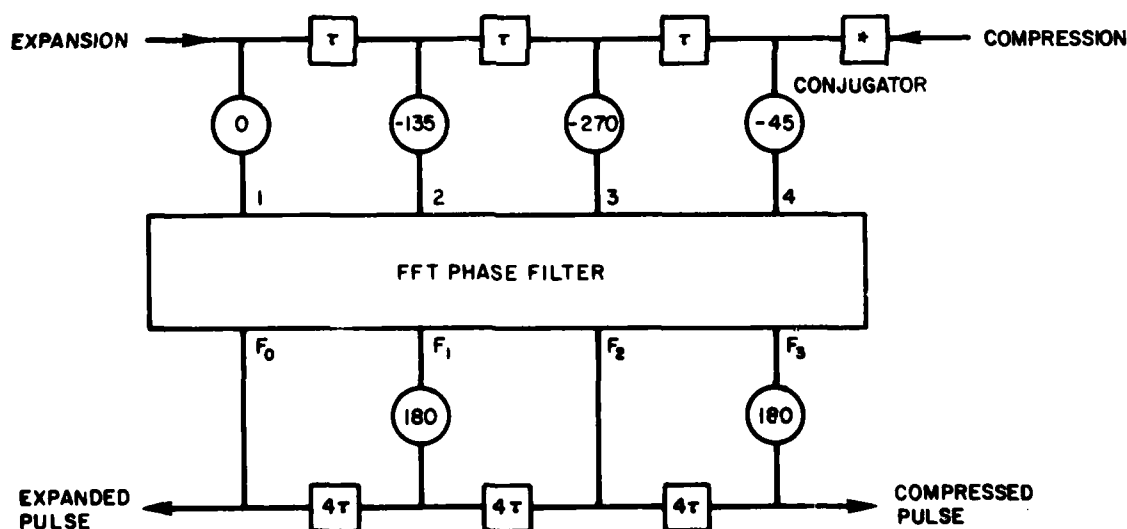


Fig. 12 — P1 code generation and expansion using FFT

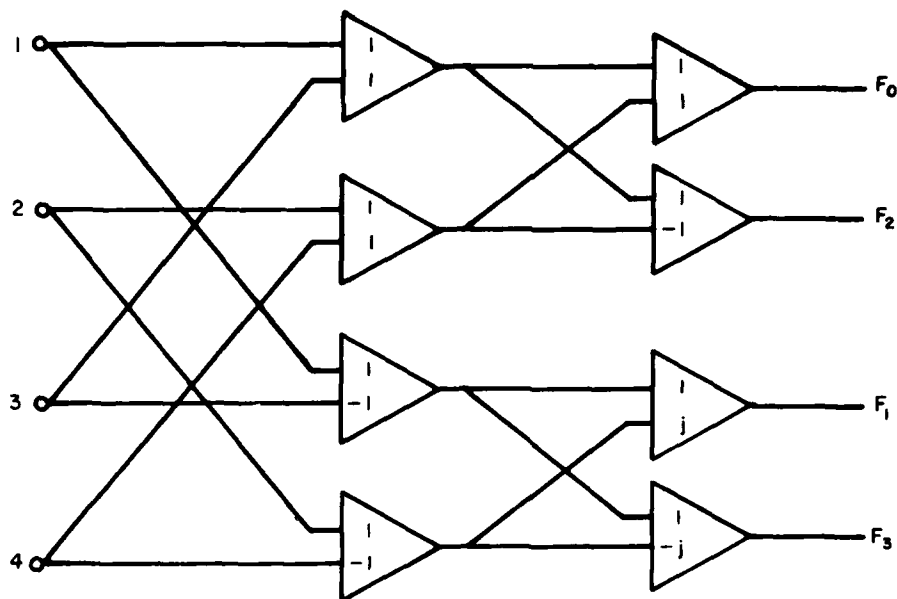


Fig. 13 — FFT phase filter

Comparison of Doppler Responses and Effects of Weighting

In this section we compare the doppler responses of the various 100-element codes by examining the doppler variation of the peak compressed signal, the peak sidelobes or secondary maxima, and the image signal. The image signal is due to the polyphase codes being derived from a Nyquist rate sampling of the step-chirp or linear-chirp phase characteristics. These are illustrated in Fig. 14 for a Frank-coded receive waveform having a normalized doppler frequency of -0.05 .

The doppler behavior of the Frank, P1, and P2 codes is the same and is shown in Fig. 15, where the cyclic variation of the peak amplitude is evident. Also, there is a cyclic behavior of the secondary maxima and the envelope of the peak signal response every 0.1 in normalized doppler. This doppler corresponds to a range doppler coupling of ten range cells for the 100-element code, which is the equivalent duration of one phase or frequency group. These secondary maxima are nearly the same as those which occur for an analog step-chirp compressed pulse having the same doppler-shifted input waveform [4]. Figure 15, except for the rapid cyclic behavior, is similar to Fig. 8.28 in [4]; however, the peak response in Fig. 15 does not fall off as fast with doppler. This is attributed to our sampling the received Frank code once per code element. Also, our secondary maxima and image signal include the 0-doppler values.

The P3 and P4 codes also have the same doppler behavior; this is shown in Fig. 16, where it is evident that the secondary-maximum sidelobes are generally much less than those for the Frank, P1, and P2 codes shown in Fig. 15. At zero doppler, the P3 and P4 codes have sidelobes that are approximately 4 dB higher than those of the Frank, P1, and P2 codes. The compressed pulse for the P3 or P4 code having a doppler shift of -0.05 is shown in Fig. 17; it should be compared with the Frank, P1, and P2 compressed pulse in Fig. 14.

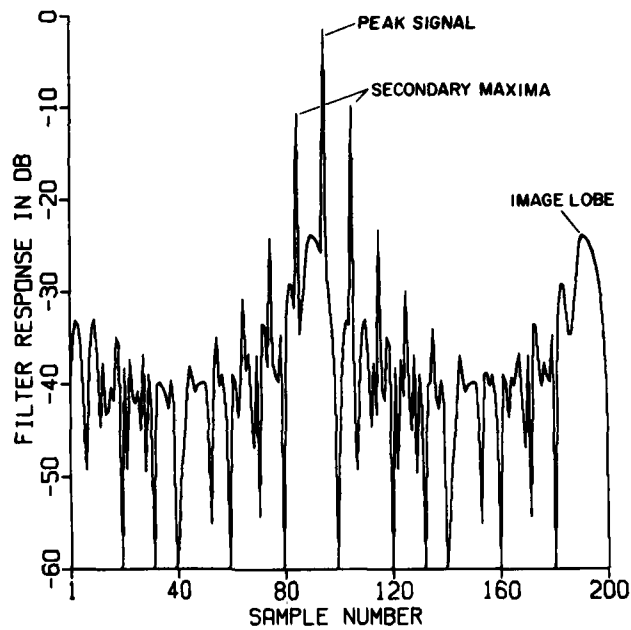


Fig. 14 — Compressed pulse of 100-element Frank code,
doppler = -0.05

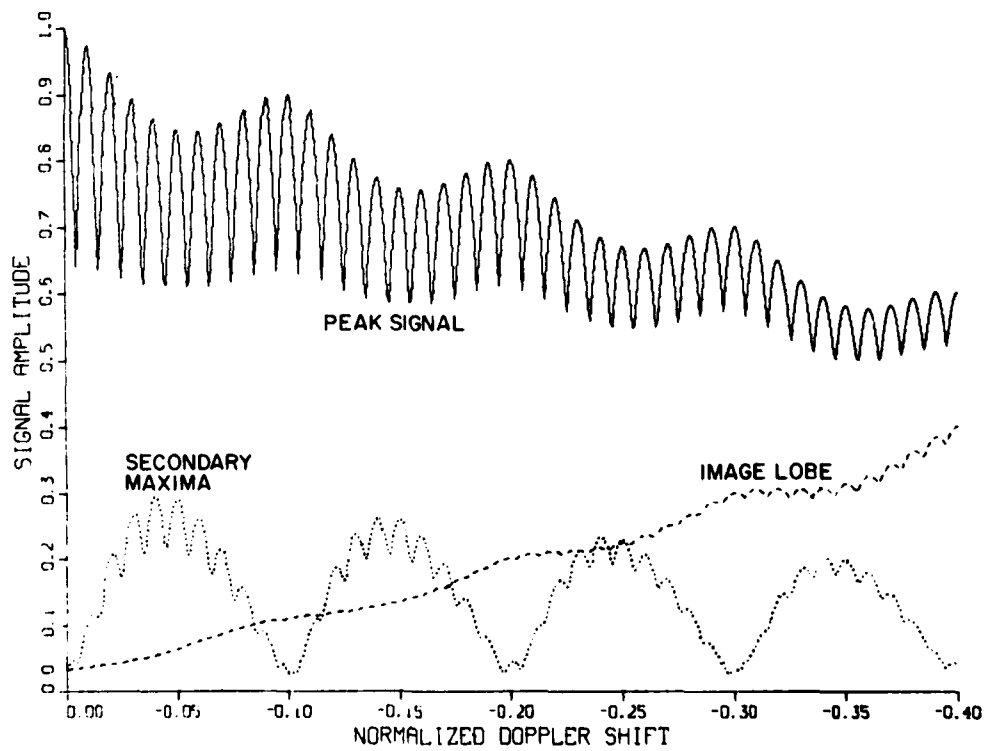


Fig. 15 — Doppler properties of 100-element Frank,
P1, and P2 codes

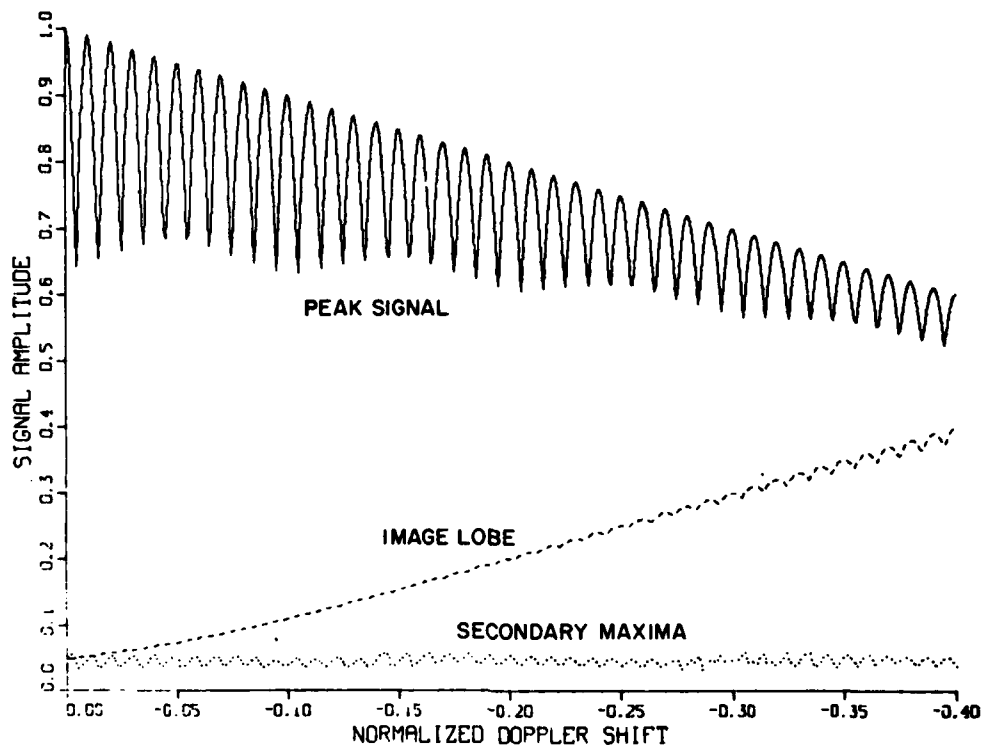


Fig. 16 — Doppler properties of 100-element P3 and P4 codes

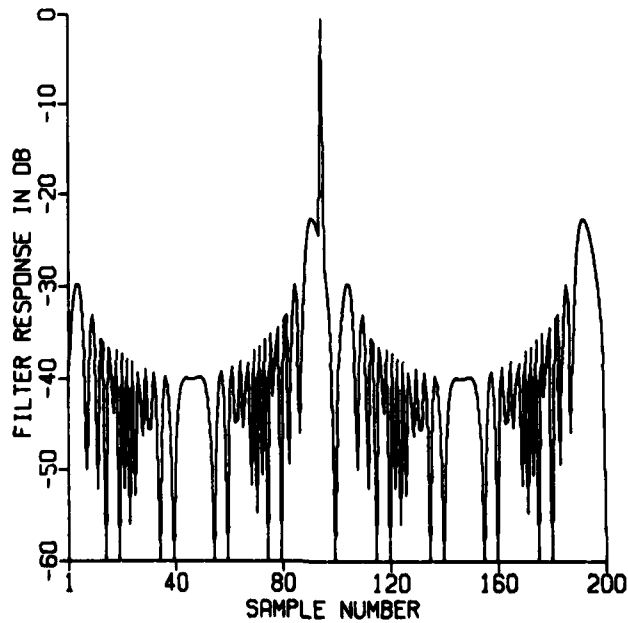


Fig. 17 — Compressed pulse of 100-element P4 code,
doppler = -0.05

The effects of weighting, using a cosine on a pedestal of 0.2, are depicted in Fig. 18 for the Frank, P1, and P2 codes (Case 1) and in Fig. 19 for the P3 and P4 codes (Case 2). Figures 20 and 21 show the compressed pulses for the weighted Case 1 and Case 2 codes. Parts (a) and (b) of these figures show normalized doppler frequencies of 0.0 and -0.05 respectively. From these figures and a comparison of Figs. 20(a), 20(b), 21(a), and 21(b) with the corresponding unweighted responses shown in Figs. 3, 14, 6, and 17, respectively, several observations may be made. First, weighting reduces the percentage cyclic variation of the compressed pulse peak with doppler. Second, weighting increases the ratios of the peak signal to the image lobe, the mean-squared sidelobes, and, to a lesser extent, the secondary maxima. Another aspect of weighting is that it can be shown to reduce the fluctuation of the compressed pulsewidth as the doppler varies.

Band-Limiting Effects on Doppler Responses

In this section we describe the effects of band limiting prior to pulse compression. We previously described how band limiting acts as an adverse amplitude weighting on the Frank and P3 codes but improves the P1, P2, and P4 symmetrical codes.

The behavior of the polyphase codes was compared in the presence of band limiting. We simulated the band-limiting effect by oversampling the received coded waveform by a factor of five to approximate the analog received waveform and then filtering this waveform with a five-sample sliding-window average. The inputs to the pulse compressor were then taken, using every fifth sample. The particular set of inputs is therefore dependent on the starting time. The outputs of the compression filter were computed for the five sets of input data, corresponding to different sampling times within the subpulse width of the coded element. The data were averaged and are shown in Figs. 22, 23, and 24 for the Frank, P2, and P4 codes, respectively, for normalized doppler frequencies of 0.0 and -0.05 . The results for the P3 and P1 codes were similar to those for the Frank and P2 codes, respectively, and are not shown. In Figs. 22(a), 23(a), and 24(a) showing the zero doppler cases, the peak responses are each reduced approximately 2.4 dB. However, for the Frank code the secondary maxima and the image sidelobes are not reduced. Thus, it is seen that, in the presence of band limiting, the Frank-code compressed-pulse degrades. In Figs. 23(a) and 24(a) we see that the secondary maxima and image sidelobes are approximately 5 dB lower, with the result that the peak signal to sidelobe ratio is improved. In Figs. 22(b), 23(b), and 24(b), we show the same codes having a normalized doppler shift of -0.05 . Comparing Fig. 22(b) with Fig. 14 for the Frank code, we see that the sidelobe levels are approximately the same although the peak signal is reduced by nearly 4 dB. This again shows that the Frank code is degraded in the presence of band limiting. For the P2 code in Fig. 23(b), the ratio of the peak signal to secondary maxima is the same as it is for no band limiting (this ratio is the same as that for the Frank code shown in Fig. 14); however, the ratio of the peak signal to the image lobe has improved by approximately 3 dB. In Fig. 24(b), showing the band-limited P4 coded waveform having a doppler shift of -0.05 , the ratio of the peak signal to the image lobe is also improved by approximately 3 dB compared to the case shown in Fig. 17 for no band limiting.

From these results and prior comments, it is seen that, for zero and nonzero doppler shifts, the Frank and P3 codes degrade in the presence of band limiting. On the other hand, the symmetrical P1, P2, and P4 codes improve mainly in terms of the ratios of the peak signal to the image lobe and the mean-squared sidelobes. The peak signal to secondary maxima ratio is improved by several decibels for zero doppler, and for higher dopplers the ratio is approximately the same. The large secondary maxima of the Frank, P1, and P2 codes which occur at the higher doppler frequencies are not present with the P3 or P4 codes.

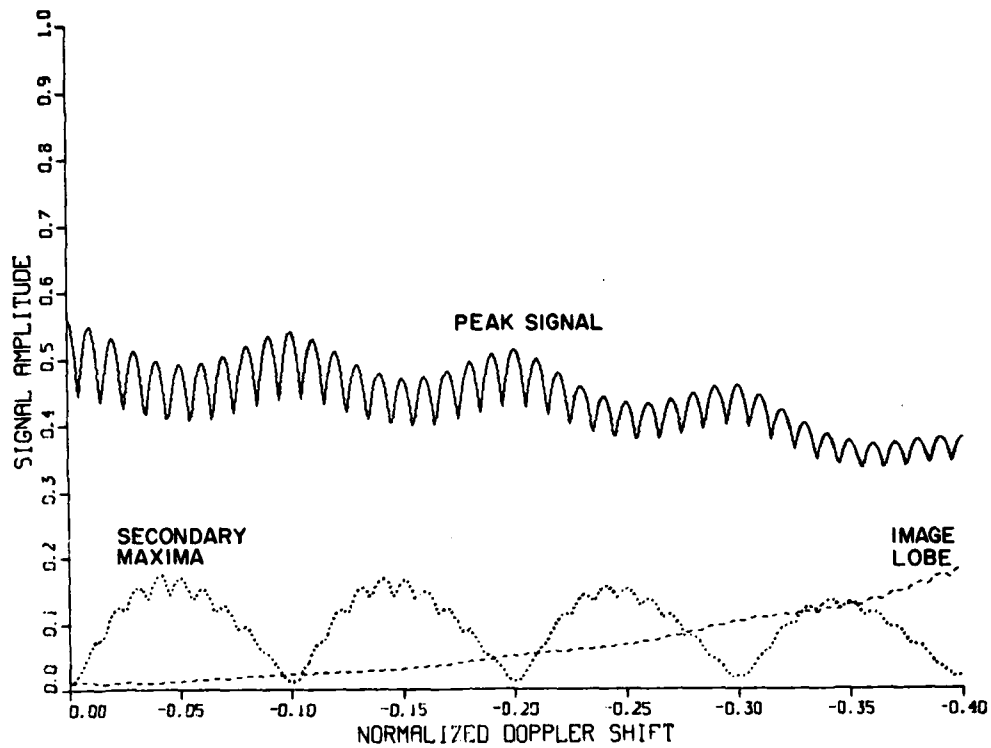


Fig. 18 — Doppler properties of weighted 100-element Frank, P1, and P2 codes

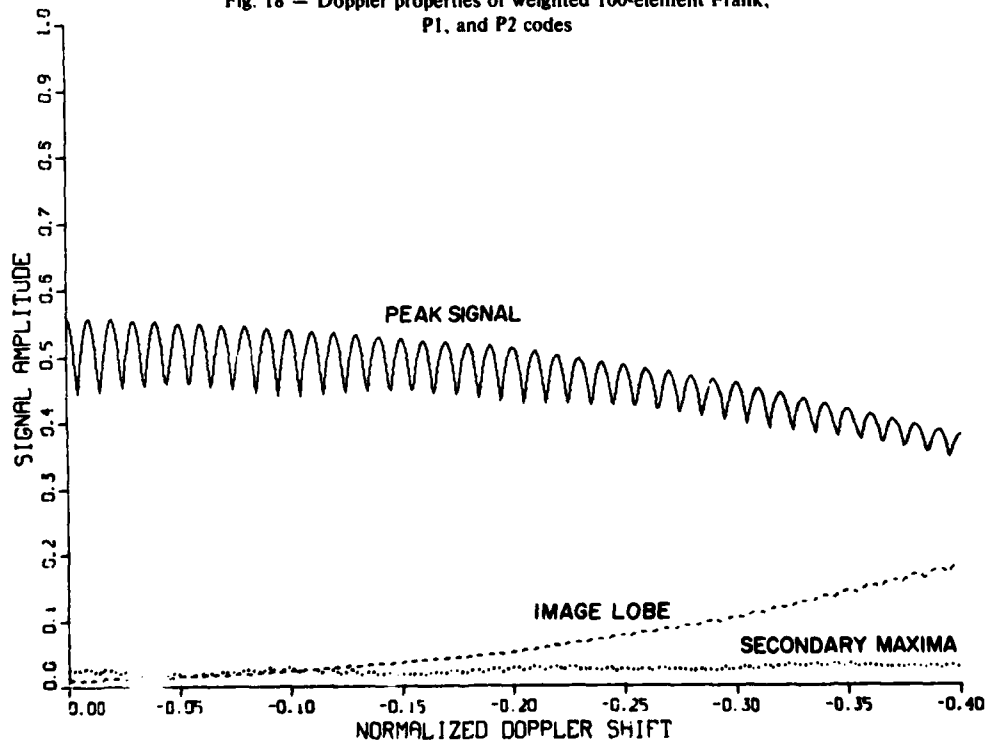


Fig. 19 — Doppler properties of weighted 100-element P3 and P4 codes

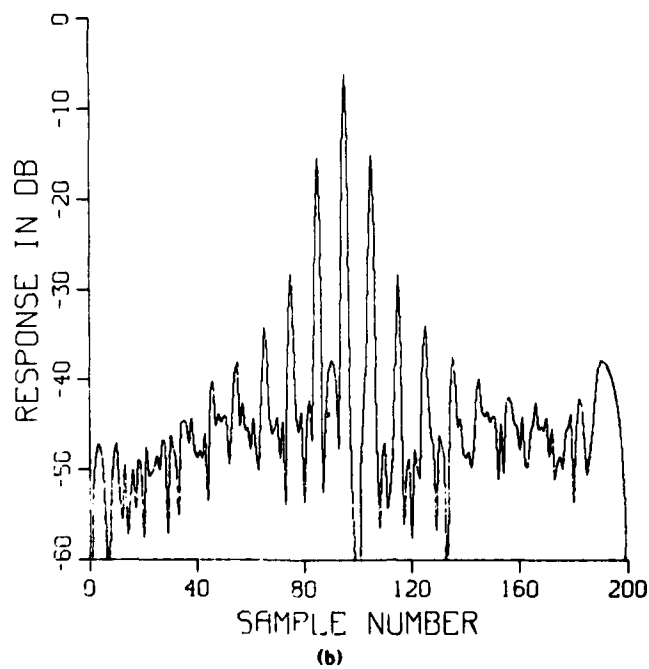
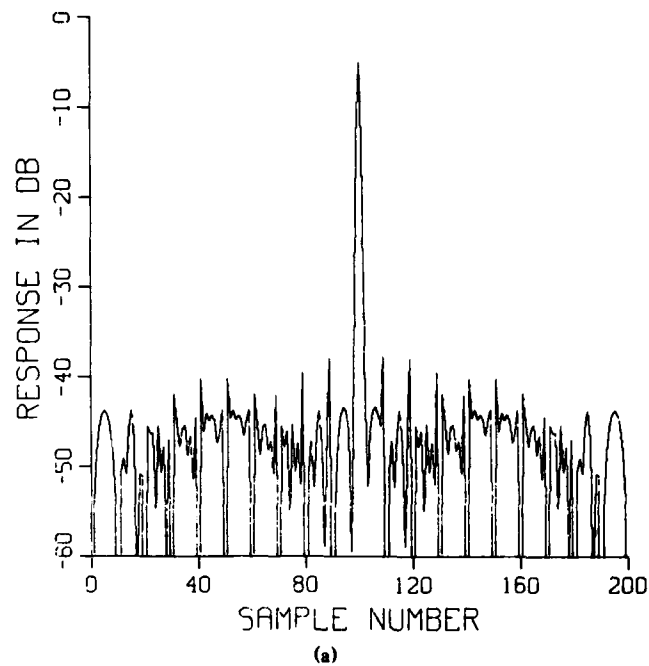


Fig. 20 - Compressed pulse of weighted 100-element Frank, P1, and P2 codes:
(a) doppler = 0.0, (b) doppler = -0.05

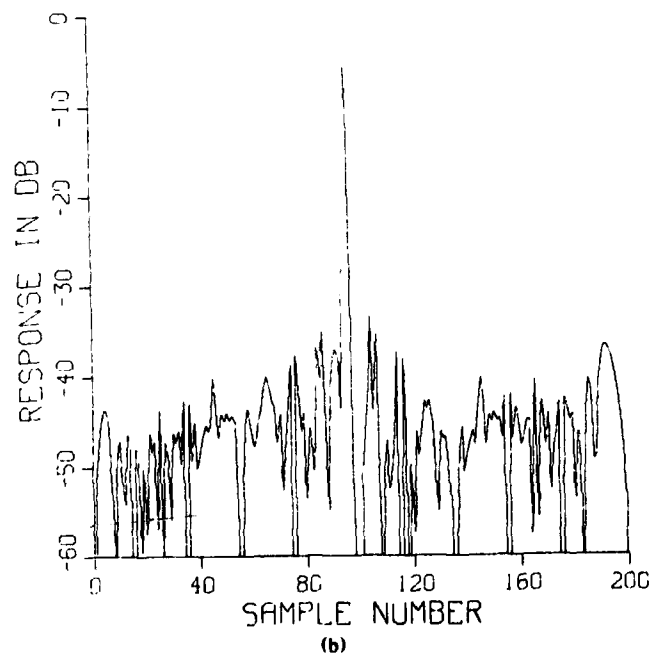
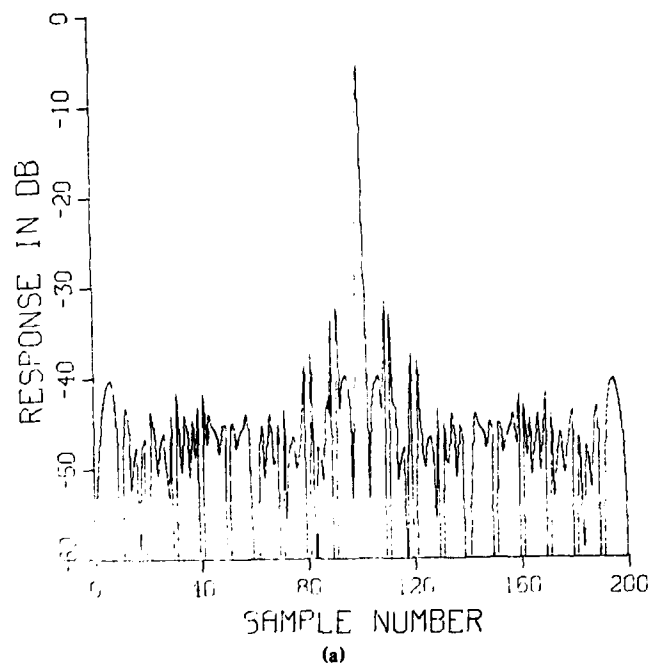


Fig. 21 — Compressed pulse of weighted 100-element P3 and P4 codes:
(a) doppler = 0.0, (b) doppler = -0.05

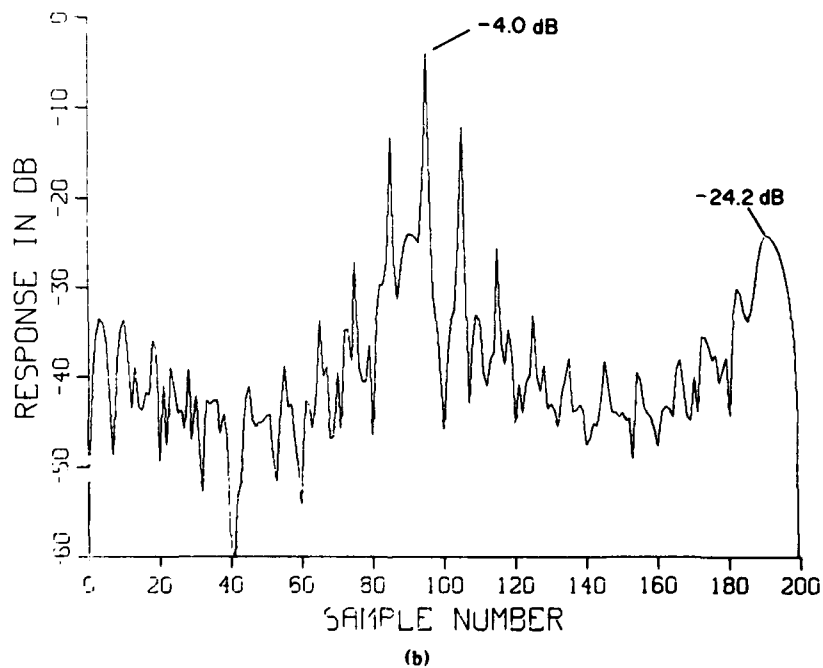
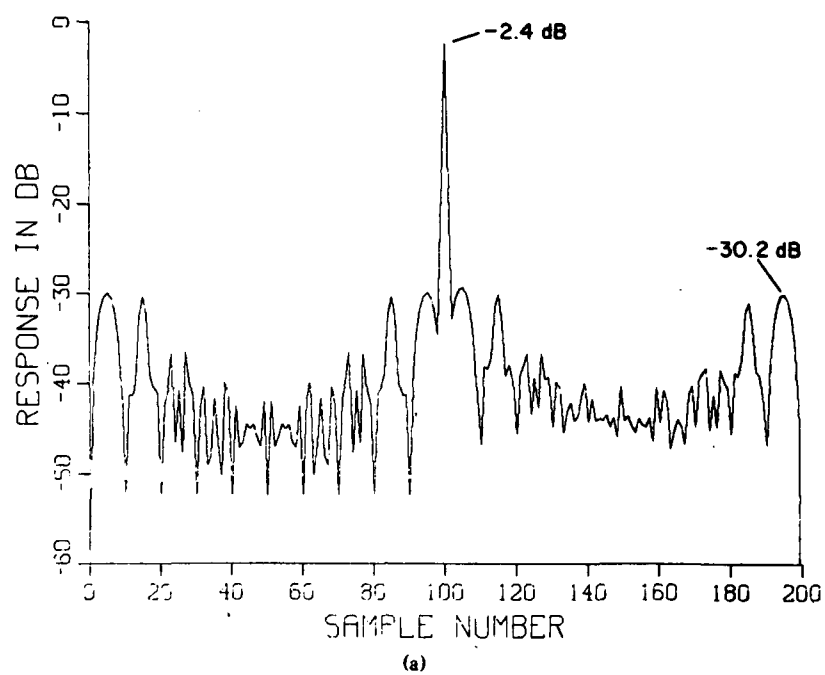


Fig. 22 — Average compressed pulse of 100-element Frank code after band limiting: (a) doppler = 0.0, (b) doppler = -0.05

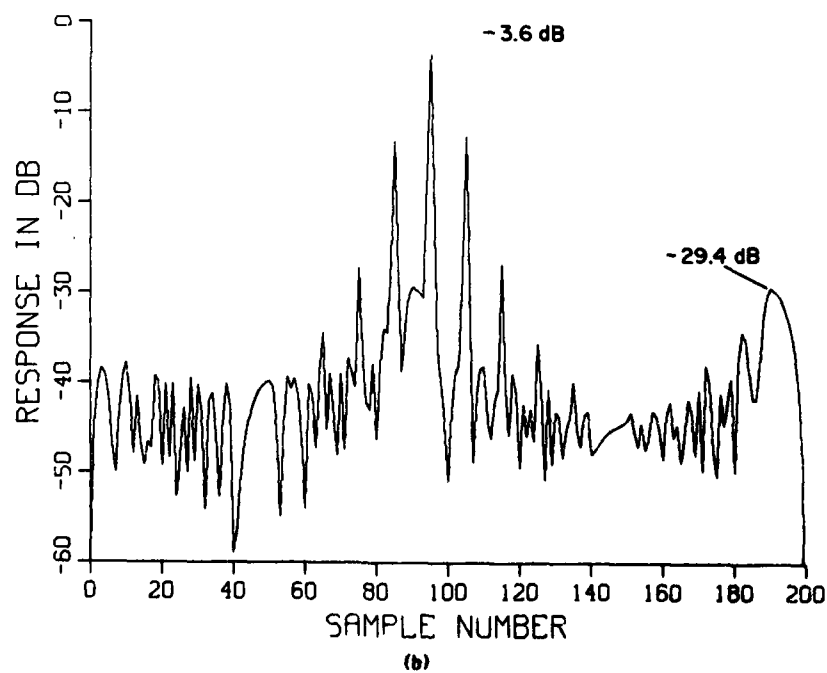
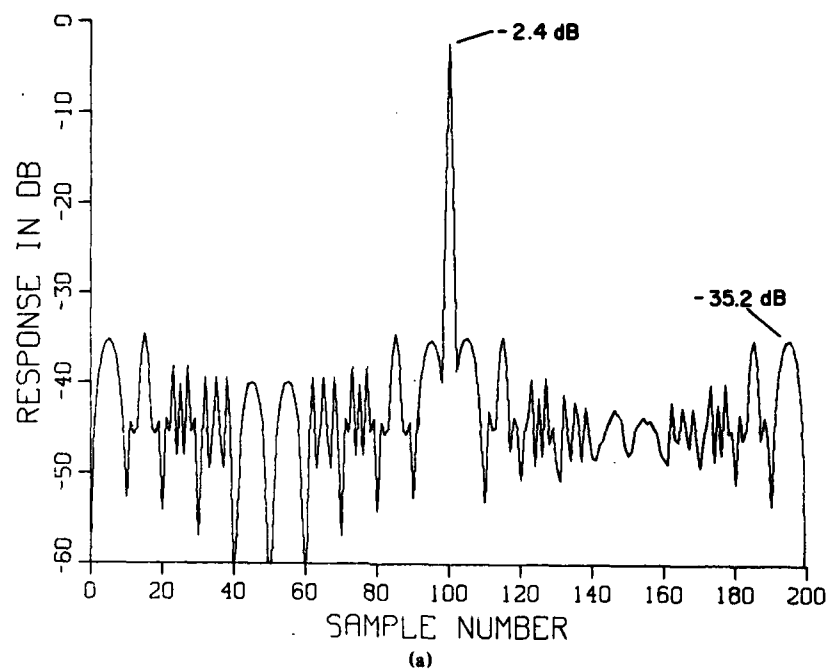


Fig. 23 — Average compressed pulse of 100-element P2 code after band limiting: (a) doppler = 0.0, (b) doppler = -0.05

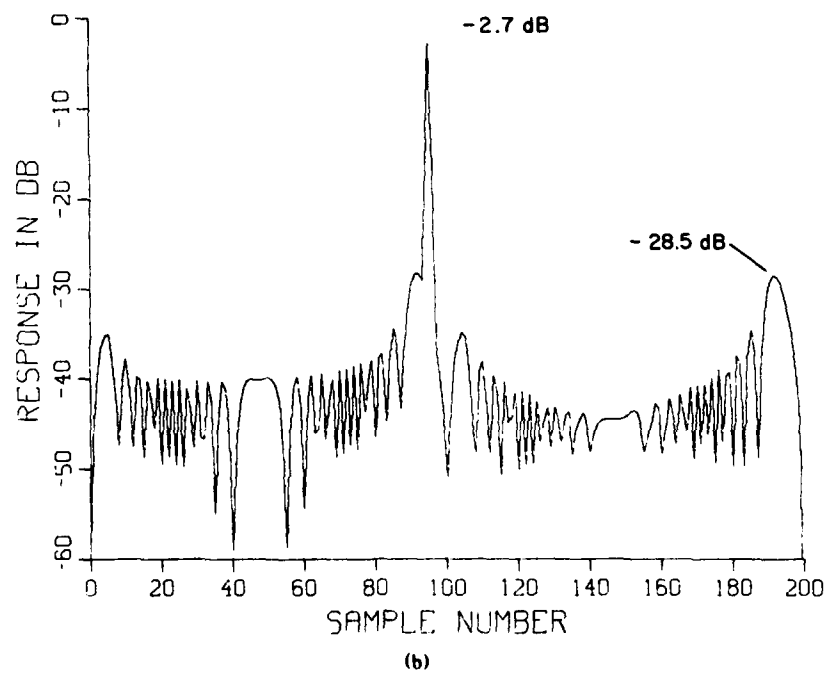
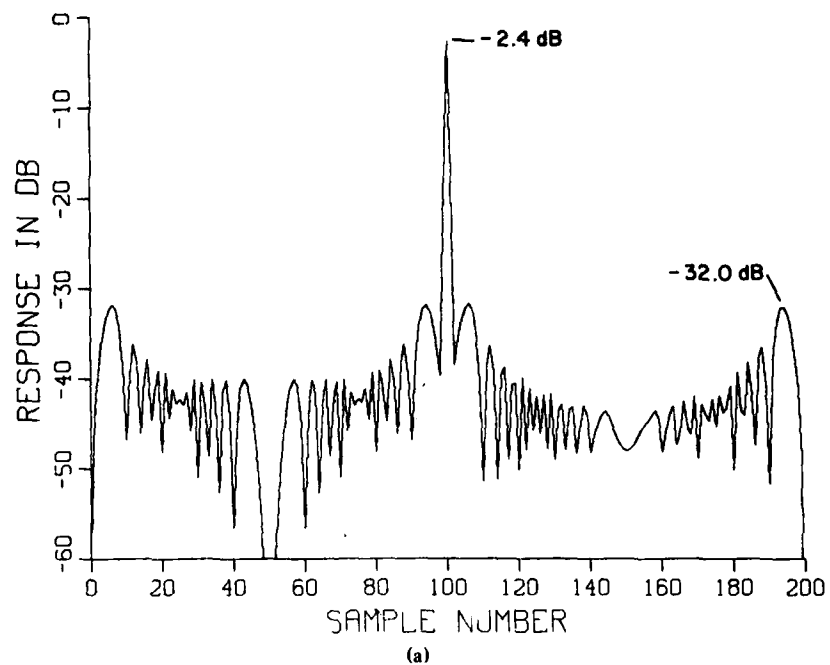


Fig. 24 — Average compressed pulse of 100-element P4 code after band limiting: (a) doppler = 0.0, (b) doppler = -0.05

SUMMARY

The basic properties of the Frank and the P1, P2, P3, and P4 polyphase codes were presented. It was shown how these codes may be obtained from considering the sampled phases of the step-chirp and chirp baseband waveforms. These codes can be digitally compressed by using FFT's directly or by a fast convolution technique.

The doppler properties of these waveforms were investigated in detail. It was shown that these waveforms have a cyclic loss of approximately 4 dB, which is attributed to the p discrete phases that are used. As the number of phase samples increases, this loss diminishes and the sidelobe levels approach the 13-dB level of the chirp waveform. It was shown that this loss occurs when the total phase shift across the uncompressed pulse is an odd multiple of π radians. This loss can therefore be reduced by providing a phase-compensated channel which has approximately a π phase shift across the uncompressed pulse; then, for example, the channel having the largest signal is selected. Also, it was shown that weighting reduced the cyclic variation of the peak response and stated that it reduced the variation of the pulsewidth with doppler.

The doppler responses of the P3 and P4 codes were shown to have much lower secondary maxima than the Frank, P1, and P2 codes and to have comparable image lobes. However, amplitude weighting was shown to primarily increase the ratio of the peak signal to the image lobe, the ratio of the peak signal to the mean-squared sidelobes, and, to a smaller extent, the ratio of the peak signal to the secondary maxima.

The effects of band limiting were investigated for zero and nonzero doppler-shifted waveforms, and for the symmetrical P1, P2, and P4 codes the results were found to be similar to those for amplitude weighting. For these codes, it was found that the ratios of the peak signal to the image lobe, the mean-squared sidelobes and, to a lesser extent, the secondary maxima are improved. However, for the unsymmetrical Frank and P3 codes these ratios are degraded.

The P4 code, in addition to being tolerant of band limiting, was shown to provide better doppler tolerance than the other codes in the presence of relatively large doppler shifts. However, for small normalized doppler shifts of less than approximately $1/(2p)$, the P1 or P2 codes have lower peak sidelobes. The preferred code therefore depends on the expected doppler shifts.

ACKNOWLEDGMENT

The assistance of Mrs. F. C. Lin in obtaining the computer plots is gratefully acknowledged.

REFERENCES

1. B.L. Lewis and F.F. Kretschmer, Jr., "A New Class of Polyphase Pulse Compression Codes and Techniques," *IEEE Trans. Aerosp. Electron. Syst.*, AES-17, 364-372 (May 1981).
2. F.F. Kretschmer, Jr., and B.L. Lewis, "Polyphase Pulse Compression Waveforms," NRL Report 8540, Jan. 5, 1982.
3. B.L. Lewis and F.F. Kretschmer, Jr., "Linear Frequency Modulation Derived Polyphase Pulse-Compression Codes and an Efficient Digital Implementation," NRL Report 8541, Nov. 2, 1981.
4. C. Cook and M. Bernfield, *Radar Signals: An Introduction to Theory and Applications*, Academic Press, New York, 1967.
5. F.E. Nathanson, *Radar Design Principles: Signal Processing and the Environment*, McGraw-Hill, New York, 1969.
6. R.L. Frank, "Polyphase Codes With Good Nonperiodic Correlation Properties," *IEEE Trans. Inf. Theory*, IT-9, 43-45 (Jan. 1963).

END

DATE
FILMED

12-82

DTIC